IJIRCCE

e-ISSN: 2320-9801 | p-ISSN: 2320-9798

INTERNATIONAL JOURNAL OF INNOVATIVE RESEARCH

IN COMPUTER & COMMUNICATION ENGINEERING

Volume 12, Issue 3, March 2024

INTERNATIONAL STANDARD SERIAL NUMBER INDIA

Impact Factor: 8.379

International Journal of Innovative Research in Computer and Communication Engineering

| e-ISSN: 2320-9801, p-ISSN: 2320-9798| www.ijircce.com | |Impact Factor: 8.379 | Monthly Peer Reviewed & Referred Journal |

|| Volume 12, Issue 3, March 2024 ||

| DOI: 10.15680/IJIRCCE.2024.1203009 |

Stabilization and Monitoring of Gait Parameters Using Machine Learning

V. Yamini, Dr. S. Sargunavathi

P.G. Student, Applied Electronics, Sriram Engineering College, Perumalpattu, Tamilnadu, India

Associate Professor, Applied Electronics, Sriram Engineering College, Perumalpattu, Tamilnadu, India

ABSTRACT: A gait pattern that doesn't cause falls is termed a stable gait. Monitoring the gait stability continuously is enviable for evaluating balance control and fall risk. Particularly, reliable surveillance is essential for aged people due to the decline of their physical fitness to reduce the fall effects. In this project, a monitoring system that precedes human subjects by utilizing sensors on wearable footwear, which are fused with a gyroscope sensor, accelerometer sensor, and temperature sensor for capturing specific data while walking, is proposed. Sensors are embedded with an ESP32 microcontroller that sends the gathered data from sensors to an open-source IDE utilizing MQTT protocol via WiFi. For predicting gait instability, a Machine Learning (ML) algorithm like Random Forest (RF) is utilized. For analogizing with real-time output data, approximately 985 datasets of accelerometer sensors and gyroscope sensors are gathered. For providing fall-risk evaluation, real-time data from a pair of instrumented footwear are gathered to monitor gait stabilization. The real-time normal and abnormal datasets are gathered in data collection. These datasets are classified as training datasets and testing datasets in which testing datasets are kept separate and training datasets train the model. Next, for pre-processing the data, a data pre-processing technique is utilized. For training the pre-processed datasets, a random forest ML algorithm is utilized. During training time, multiple Decision Trees (DTs) are constructed by utilizing classification approaches. Predicted parameters together with gait instability (Yes or No) are exhibited in mobile applications. Lastly, when gait instability is determined, a buzzer sound is activated in the wearable device.

KEYWORDS: Wearable sensors, gait, machine learning, prediction of accuracy

I. INTRODUCTION

The advent of diseases like low extremity diseases or else motor nerve dysfunction has elevated as people become old, which results in an augmented rate of aged adults falling on flat ground. During a one-year interval, about 32% of community-dwelling old men more than 75 years of age fall at least once. Moreover, 24% of these individuals bear severe injuries. The medical expenses in relation to falls are extensive in the United Kingdom (UK). It is reported that fall-related injuries in grown-ups over 60 years cost over £981 million per annum. Overall healthcare costs accountable to elderly adult falls vary from $48 million in Alaska to $4.4 billion in California. As per the report in 2014, Medicare costs for elderly falls vary from $22 million in Alaska to $3 billion in Florida. Lifetime medical spending for fall-related injuries varies from $68 million in Vermont to $2.8 billion in Florida. In the growing number of elderly people, falling has become an extensive issue.

Hence, owing to safety measures' deployment in higher-risk work environments, nursing homes, as well as hospitals, fall risk detection and recognition is developing. Through gait analysis, a person's walking pattern could be via the progress of disorders, encompassing dementia, stroke, arthritis, Parkinson's disease, et cetera. In physical status as well as fall risk, gait could act as a marker of changes. The behavioral characteristics of the human body's lower limbs in the upright walking process are known as the human body's gait. Generally, a normal human gait cycle wants to encounter the characteristics of natural, labor-saving, periodicity, and coordination of the legs. Before the human body falls, abnormal gait can grow. An abnormal gait might be caused by several possibilities. Flat ground fall prevention strategies and lower limb training regimens are considerably guided by abnormal gait patterns' identification and evaluation in the medical rehabilitation field.For mitigating the flat ground fall risk, proper preventive measures could be suggested by monitoring the elderly patients' gait patterns. The variations in the gait pattern might not be precisely recognized or else quantified by human vision. Thus, in the biomechanics as well as healthcare literature, automatic gait recognition utilizing computer vision has turned into a viral topic recently.
For obtaining gait kinematics information, encompassing velocity, acceleration, and angles of the joints regarding Kinect skeletal tracking sequences, computer-vision technology is utilized. Numerous interdependent measures are involved in the gait analysis and may be complex to understand owing to a huge amount of data along with their inter-relations. Furthermore, in off-line data analysis, a considerable amount of labor is needed.

| e-ISSN: 2320-9801, p-ISSN: 2320-9798| www.ijircce.com | |Impact Factor: 8.379 | Monthly Peer Reviewed & Referred Journal |

|| Volume 12, Issue 3, March 2024 ||

| DOI: 10.15680/IJIRCCE.2024.1203009 |

II. RELATED WORKS

Zhuo Chen [1] presented a mobile robot-supported gait monitoring as well as dynamic margin of stability estimation, which predicted a MoS monitoring system consisting of a mobile robot along with an instrumented insoles pair in which each insole embedded an array of pressure sensors as well as an IMU. For estimating foot poses as well as the body CoM in the existence of measurement uncertainties along with noises, Kalman filter-centered methodologies were designed for fusing the data as of the sensors. T.J. Buurke [2] introduced updated equations for the mediolateral margin of stability in temporally symmetric as well as asymmetric gait that included the single support times of both legs. The association betwixt bilateral single support times as well as the mediolateral margin of stability in symmetric, asymmetric, along with adaptive human gait was identified centered on these equations. K. Karamanidis [3] presented the work for determining whether age-associated muscle weakness reduces aged adults' potential to utilize systems accountable to sustain dynamic stability subsequent to forward falls. Isometric maximal voluntary plantarflexion along with knee extension contractions on a dynamometer were performed by all subjects for analyzing the abilities of leg-extensor muscle-tendon units. A. F. Ambrose [4] introduced risk factors for falls amongst aged persons, thus analyzing the main causes of mortality as well as morbidity in older adults. Moderate to severe injuries, loss of freedom, fear of falling, along with fatality in those patients were caused by falls. S. Whitney [5] presented the dynamic gait index associated with self-reported fall history in persons with vestibular dysfunction that studied the relationship betwixt gait instability and fall history in persons with vestibular disorders. L. Salonen [6] devised eye diseases along with impaired vision as probable risk factors for persistent falls in older persons that carried out a systematic review regarding the relationships betwixt eye diseases or else impaired vision and recurrent falls risk in older people. J.M. Hausdorff [7] introduced gait variability as well as fall risk in community-living aged people, who tested the hypothesis that elevates gait variability and predicts falls among community-living aged people attending an outpatient clinic. C.S. Florence [8] presented medical costs of fatal along with nonfatal falls in aged persons to evaluate medical expenditures attributable to aged individual falls by employing a scheme that could be updated yearly for tracking these expenditures over time. S. Bruijn [9] assessed human locomotion's stability for the detection of persons at falling risk because of an unstable gait by measuring the parameters' variability. A. Hof [10] presented the dynamic stability condition to gauge the CoM's position as well as its velocity times a factor of 1/g within the BoS for naming this vector quantity extrapolated from the centre of mass position. Here, an effective technological solution for gait stabilization utilizing an ML algorithm provided high accuracy.

Here, a monitoring system consisting of sensors in wearable footwear is proposed, and the ESP32 is connected to get the data from sensors. ML is used for fusing the data from these sensors for evaluating foot pose parameters via MQTT protocol during walking. The experiments are done for predicting the human subject's parameters in overground walking for real-time gait. RF is a commonly used ML algorithm that is used for determining the results from the collected parameters that pose the highest accuracy based on voting by averaging the DT. After validation and evaluation, the prediction of gait instability says whether Yes or No. If yes, then the buzzer will sound, and fall fall-down notification will be sent to the caretaker along with parameters.

Designing and performing RF algorithms, which analyze vast amounts of data quickly and accurately using DTs with the highest accuracy for elderly people who face gait, is the major contribution of this study. The instrumented footwear's inclusion assists in monitoring the real-time gait and provides fall-risk assessment during walking. The remaining paper is structured as: the proposed system together with the experimental protocol is described in Section III.

III. METHODOLOGY

To capture the specific data while walking, fall detection requires an instrumented wearable footwear subsystem, which contains a gyroscope sensor, accelerometer sensor, and temperature sensor. Sensors are fused with an ESP32 microcontroller, which sends the gathered data from sensors to an open-source IDE by utilizing MQTT protocol via WiFi. To predict gait instability, ML algorithms, such as RF are utilized. To compare with real-time output data, around 985 datasets of accelerometer sensors and gyroscope sensors are collected. Real-time data from a pair of instrumented footwear are collected to monitor gait stabilization for rendering fall-risk assessment. The real-time dataset is collected by the data collection. Collected datasets are separated as training datasets and testing datasets in which testing datasets are kept separate and training datasets train the model. After that, to pre-process the dataset, data pre-processing techniques are utilized. To train the pre-processed datasets, an RF ML algorithm is utilized. During training time, multiple DTs are constructed utilizing classification approaches. Inmobile application is displayed by the predicted

| e-ISSN: 2320-9801, p-ISSN: 2320-9798| www.ijircce.com | |Impact Factor: 8.379 | Monthly Peer Reviewed & Referred Journal |

|| Volume 12, Issue 3, March 2024 ||

| DOI: 10.15680/IJIRCCE.2024.1203009 |

parameters along with gait instability (Yes or No). Lastly, buzzer sounds are activated in wearable devices while gait instability is determined.

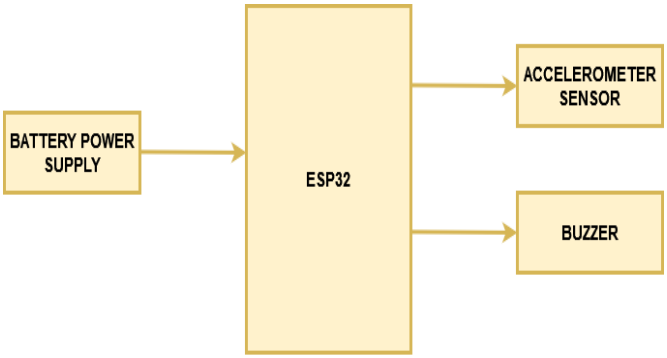

Fig.1. Block Diagram of Proposed System

A. SYSTEM ARCHITECTURE DESIGN AND IMPLEMENTATION SCHEME

The gait stabilization measurement system consists of wearable footwear. Each of the subsystems and the implementation scheme are described in this section.

1. Wearable Footwear Subsystem

Customized footwear consists of an accelerometer sensor that captures the motion data acting in a human subject, such as the x, y, as well as z-axes, measuring a magnitude of normal and abnormal conditions. Regarding the x, y, as well as z-axes of normal and abnormal conditions and measuring parameters like stride length, step time, step length, step velocity, stride time, along with step count, the gyroscope angular velocity sensor detects the changes in rotation angle per unit of time. The temperature sensor measures the room temperature. Battery power is composed of an ESP32 microcontroller embedded with sensors, which sends the collected data from sensors to the open source collab through MQTT protocol through WiFi. Additionally, during gait instability, the buzzer at the microcontroller makes a sound.

2. Subsystem Communication

The instrumented footwear communicates in an open-source IDE through WiFi through MQTT Protocol and creates its own collab notebooks. By utilizing an ML algorithm, the collected data from the instrumented footwear is processed. The programs for gait analysis run through a decision RF algorithm. The parameter measurement and fall-down notification are displayed by the React native mobile application.

3. System Analysis of the software module

a. Dataset Collection

From wearable footwear, the real-time dataset is collected. Also, real-time datasets are trained with an ML algorithm, which increases inaccuracy by increasing dataset collection. For performing an ML model, data are continually fed to an open source, thus improving the availability of more labeled data and performing better. From the accelerometer and gyroscope sensors, around 1370 normal and abnormal data are collected for determination of gait stabilization in which mems are employed in accelerometer ICs, which aids in keeping its size small. By using a spring, a sequence of fixed plates on the exterior assembly and movable internal assembly are linked to the outer assembly. The movable assembly also contains plates, which create capacitors with plates of externally fixed assembly. Owing to displacement and changes in the value of different capacitors, the internal assembly moves as the system travels with acceleration. Gauging these modifications in capacitance could infer the acceleration that acts on the body, which has such multiple mems system in different names like X-axis, Y-axis, and Z-axis.

Subsequently, the acceleration renders the reading of acceleration in diverse directions as exhibited by the body. When the body of mass moves in X direction with the velocity Vx, Coriolis force is experienced by the body of mass if an angular velocity acts in the Y-direction since the way in gyroscope Coriolis effect helps in measuring rotation on the angular velocity. Coriolis force is a vector quantity that is perpendicular to the velocity in the X-direction as well as the angular velocity in the Y-direction. Next, the Coriolis force's magnitude is proportional to the body's mass, velocity, along with angular velocity. By utilizing a right-hand rule in the X-axis, Y-axis, along with Z-axis, the direction of this force can be found. In this, some rows of normal and abnormal collected data from the accelerometer and gyroscope sensor are displayed.

| e-ISSN: 2320-9801, p-ISSN: 2320-9798| www.ijircce.com | |Impact Factor: 8.379 | Monthly Peer Reviewed & Referred Journal |

|| Volume 12, Issue 3, March 2024 ||

| DOI: 10.15680/IJIRCCE.2024.1203009 |

	accel_x	accel_y	accel_z	gyro_x	gyro_y	gyro_z	time	cur_time
0	2.60	9.43	0.37	0.02	0.03	0.01	0.621	10:58:05
1	2.08	9.61	0.51	0.13	0.14	0.08	1.179	10:58:05
2	1.82	9.67	0.60	0.05	0.11	0.02	1.683	10:58:06
3	1.69	9.57	0.89	0.05	0.12	0.17	2.169	10:58:06
4	0.05	9.39	-2.10	0.56	0.20	0.00	2.718	10:58:07

Table.1. Displaying the first five rows of normal data

	accel_x	accel_y	accel_z	gyro_x	gyro_y	gyro_z	time	cur_time
0	0.01	10.27	1.13	0.23	0.51	0.04	0.593	11:07:09
1	-6.35	12.14	-7.68	0.21	1.26	0.08	1.033	11:07:09
2	2.63	9.63	0.82	0.11	0.01	0.23	1.551	11:07:10
3	3.15	9.42	0.87	0.01	0.01	0.00	2.070	11:07:10
4	2.61	9.52	0.85	0.02	0.00	0.29	2.603	11:07:11

Table.2. Displaying the first five rows of abnormal data

b. Comparison of normal and abnormal gyroscope data

To predict the fall risk assessment, the data from the gyroscope sensor are taken for calculating the gait performance in a person while walking. By measuring the angular motion in moving bodies, the changes in angles give the x, y, along with z-axis that are labeled in Table 1 and Table 2. Approximately, 1370 data were collected, and the axis comparisons are plotted in graphical representation.

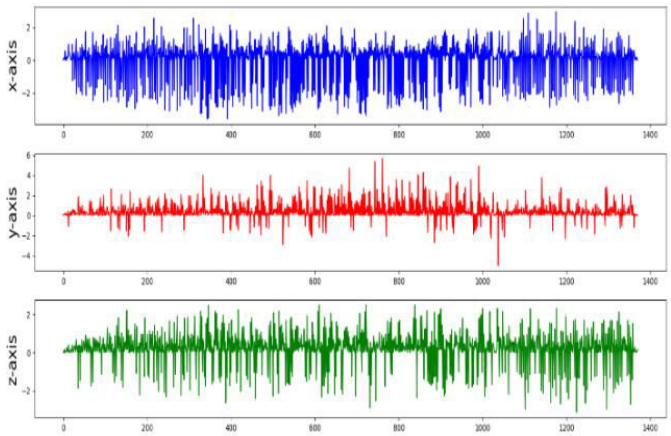

Fig.2. Normal Gyroscope sensor

| e-ISSN: 2320-9801, p-ISSN: 2320-9798| www.ijircce.com | |Impact Factor: 8.379 | Monthly Peer Reviewed & Referred Journal |

|| Volume 12, Issue 3, March 2024 ||

| DOI: 10.15680/IJIRCCE.2024.1203009 |

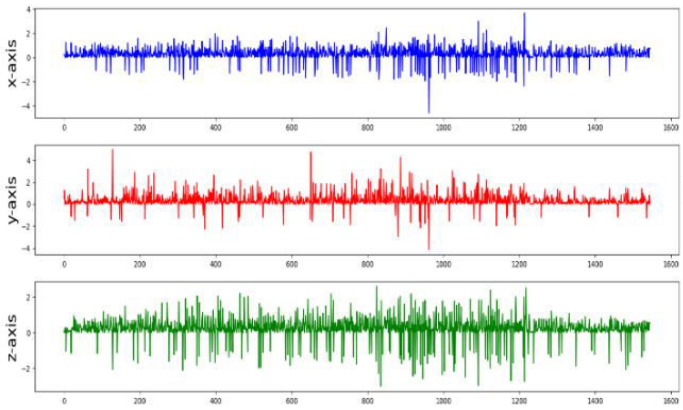

Fig.3. Abnormal Gyroscope Sensor

c. Comparison of normal and abnormal accelerometer data

The ICs that measure acceleration are called Accelerometer sensors. The change in speed (velocity) per unit of time is named acceleration, and its international (SI*) unit is M/s^2. An acceleration of 9.8 meters per second in the given direction is represented by the value of 1.0. Depending upon the direction, the acceleration values may be positive or negative. As per this, linear acceleration is calculated by the accelerometer centered on Newton's 2nd law of motion as,F=ma.Here, F represents a force applied to the object that is measured by the sensors, the mass is signified as m, and a symbolizes its resulting linear acceleration. From Table 1, the normal and abnormal data of the accelerometer are separated as a graphical representation. In order to determine the total acceleration, the magnitude of the acceleration is computed from the X, Y, along with Z-axis. The square root of the sum of each component's squares is the formula used for calculating the magnitude as Sqrt(x^2+y^2+z^2)

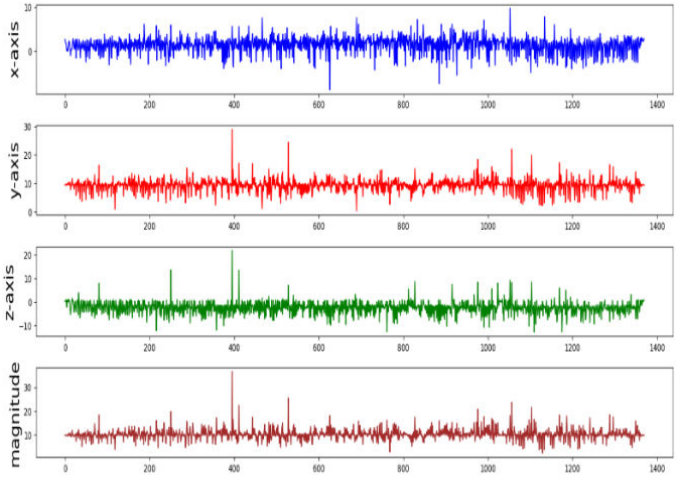

Fig.4. Normal Accelerometer Sensor

| e-ISSN: 2320-9801, p-ISSN: 2320-9798| www.ijircce.com | |Impact Factor: 8.379 | Monthly Peer Reviewed & Referred Journal |

|| Volume 12, Issue 3, March 2024 ||

| DOI: 10.15680/IJIRCCE.2024.1203009 |

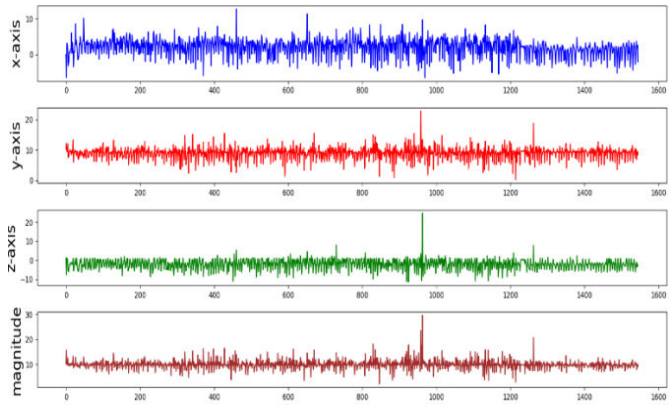

Fig.5. Abnormal Accelerometer Sensor

Computing magnitude aims to determine the absolute or relative direction in which the person moves in the sense of motion and also to predict the peak detection in magnitude. The raw acceleration data is smoothened by the peak, and then the algorithm searches for the peaks and valleys of the waveform to identify a distinct step taken. In order to determine the finest normal and abnormal steps, peak detection is done in magnitude by using scipy.signal.find_peaks.

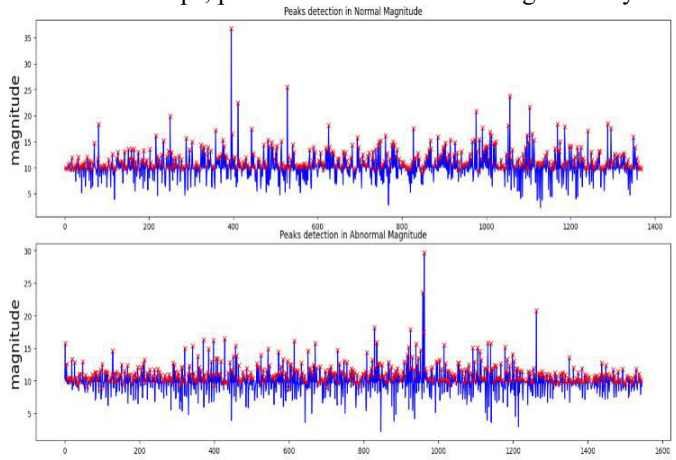

Fig.6. Peak detection in magnitude

From this peak detection, the total number of steps taken by a normal person and an abnormal person is 467 and 521, respectively. The following parameters for normal and abnormal are calculated for feature extraction by using this data.

d. Feature extraction

The Pandas is a library working with data that has flexible open-source tools. Dataframes are at the pandas' centre. Data are structured in a table or spreadsheet by utilizing this tool. There are indexes in both the rows and columns, and operations can be performed on rows and columns separately. In this, parameters like peak width, peak prominences, cadence, stride length, stride time, step velocity, step count, step length, and step time are estimated and then standard deviation and mean are calculated for x as well as y axes. Peak magnitude is required for calculating parameters. From acceleration magnitude, peaks are computed.

The time betwixt one leg's heel strike and the contralateral leg's heel strike is termed step time, which is computed as,

steptime= peaks(the acceleration magnitude).

A distance betwixt one foot's initial contact point and the opposite foot's initial contact point is termed step length. The left foot's traveled distance is the step length. The normal walking speed is fixed as 1.42 m/s and the step length is estimated as,

step length= Distance in feet/number of steps

The distance covered while the person takes 2 steps, one with each foot, and starts walking is named the stride length. Next, the stride length is computed as,

International Journal of Innovative Research in Computer and Communication Engineering

| e-ISSN: 2320-9801, p-ISSN: 2320-9798| www.ijircce.com | |Impact Factor: 8.379 | Monthly Peer Reviewed & Referred Journal |

|| Volume 12, Issue 3, March 2024 ||

| DOI: 10.15680/IJIRCCE.2024.1203009 |

stride length=Distance in feet/number of strides

The speed of travel in the specific direction of walking is defined as the step velocity, which is estimated as,

step velocity=step length/step times

The number of steps taken by a person is termed the step count, where the count will vary for every single peak. Thus, each step count is calculated regarding peak magnitude as,

step count=peaks(np diff)

Stride time is defined as the self-selected walking speed, which is approximately one second, each step takes about 0.5s. The formula utilized for calculating the stride time is,

stride time=peaks/100

The number of steps taken per unit of time is termed cadence (for example: steps per minute). This could render insights into the walking rhythms and pace. Hence, the cadence is estimated as,

cadence= 60/steps time

Peak prominences are computed as the vertical difference betwixt the peaks' height and their lowest contour line. From the highest point on the contour line that encloses the peak, the prominences are found. Next, from the peak magnitude, the mean and standard deviation of accelerometer x and y data for each step are estimated. The parameters are computed for both the normal and abnormal peak detection magnitude. In the below table, the values are predicted.

	step_times	step_length	step_velocity	step_count	stride_time	stride_length	cadence	peak_prominences	peak_widths	accel_x_mean_array	accel_y_mean_array	accel_x_std_array	accel_y_std_array	class
0	3.0	4.26	1.42	3.0	0.03	0.02	20.0	0.069197	1.740100	1.186667	9.543333	0.805495	0.119864	0.0
1	3.0	4.26	1.42	3.0	0.03	0.05	20.0	0.155288	1.718256	0.250000	9.683333	0.170489	0.054365	0.0
2	4.0	5.68	1.42	4.0	0.04	0.08	15.0	0.777494	1.152246	1.827500	9.955000	0.369526	0.311006	0.0
3	2.0	2.84	1.42	2.0	0.02	0.12	30.0	1.249351	1.210002	-0.370000	9.110000	0.630000	1.260000	0.0
4	3.0	4.26	1.42	3.0	0.03	0.14	20.0	0.279899	0.752517	0.290000	9.313333	0.078740	0.249978	0.0
...	...	...	...	...	...	...	...	...	...	...	...	...	...	...
981	3.0	4.26	1.42	3.0	0.03	15.26	20.0	1.089625	1.352863	2.746667	9.720000	0.301588	0.446393	1.0
982	5.0	7.10	1.42	5.0	0.05	15.29	12.0	3.884495	1.696147	0.068000	8.596000	2.665178	1.778590	1.0
983	2.0	2.84	1.42	2.0	0.02	15.34	30.0	0.221517	0.701032	2.270000	9.395000	0.120000	0.145000	1.0
984	3.0	4.26	1.42	3.0	0.03	15.36	20.0	2.486621	4.910564	-0.830000	8.866667	1.904328	1.335224	1.0
985	4.0	5.68	1.42	4.0	0.04	15.39	15.0	0.551301	0.935413	2.025000	8.982500	1.144825	1.270637	1.0

986 rows × 14 columns

Table.3. Displaying the calculated parameters

For finding the normal and abnormal conditions, the gathered parameter datasets are expressed in statistical form for achieving the total count, mean, std, min, and max values.

	step_times	step_length	step_velocity	step_count	stride_time	stride_length	cadence	peak_prominences	peak_widths	accel_x_mean_array	accel_y_mean_array	accel_x_std_array	accel_y_std_array	class
count	986.000000	986.000000	9.860000e+02	986.000000	986.000000	986.000000	986.000000	986.000000	986.000000	986.000000	986.000000	986.000000	986.000000	986.000000
mean	2.945233	4.187592	1.420000e+00	2.945233	0.029493	7.253976	22.644886	2.086525	1.745641	1.691580	9.117716	1.241677	1.102511	0.527383
std	1.086822	1.545287	4.443146e-16	1.086822	0.010858	4.265891	6.713964	3.205827	1.869200	1.494782	1.207976	0.866232	1.086831	0.499503
min	2.000000	2.840000	1.420000e+00	2.000000	0.020000	0.010000	6.000000	0.000282	0.530038	-3.110000	4.775000	0.000000	0.000000	0.000000
25%	2.000000	2.840000	1.420000e+00	2.000000	0.020000	3.945000	20.000000	0.684121	0.778914	0.750000	8.286750	0.544540	0.444990	0.000000
50%	3.000000	4.260000	1.420000e+00	3.000000	0.030000	7.265000	20.000000	1.944452	1.241139	1.666667	9.201667	1.102756	1.065000	1.000000
75%	3.000000	4.260000	1.420000e+00	3.000000	0.030000	10.917500	30.000000	4.016107	1.923758	2.667500	9.747250	1.784296	1.840489	1.000000
max	10.000000	14.200000	1.420000e+00	10.000000	0.100000	15.390000	30.000000	32.695301	13.017822	8.235000	19.015000	5.980000	9.955000	1.000000

Table.4. Statistical representation of parameter

e. Normalizing the data

The scaling approach applied for data preparation for varying the numeric columns' values in the dataset to utilize a common scale is named normalization. Since features are in diverse ranges, normalization is performed. Thus, normalization is mathematically computed by,

| e-ISSN: 2320-9801, p-ISSN: 2320-9798| www.ijircce.com | |Impact Factor: 8.379 | Monthly Peer Reviewed & Referred Journal |

|| Volume 12, Issue 3, March 2024 ||

| DOI: 10.15680/IJIRCCE.2024.1203009 |

Xn=(X-Xminimum)/(Xmaximum-Xminimum)
Here,
Xn= Value of normalization
Xmaximum=Maximum value of a feature
Xminimum=Minimum value of a feature
There is a model dataset that has maximal and minimal values. For normalizing the model, values are shifted as well as rescaled in order that their range varies betwixt 0 and 1. This has two cases: if the X value is minimal in the formula, the numerator's value is 0; therefore, normalization is also 0. Similarly, if the X value is maximal, the normalization is 1. Gait stabilization is determined by utilizing this normalizing approach. The condition is a normal condition when 0 occurs and an abnormal condition when 1 occurs.

f. Training and Testing Data
The data are partitioned for training and testing by normalizing the dataset. For training purposes, the training dataset is used, which is named as train model. For testing purposes, the testing dataset is used, which is named as evaluate model. From a total of 986 datasets, 788 data are split for training as well as the remaining 198 data for testing purposes, respectively (80% for training and 20% for testing the data). Primarily, to train the dataset, the training dataset is inputted to ML algorithms. This changes according to whether we are utilizing a supervised or else unsupervised learning algorithm. In unsupervised learning, the training data consists of unlabeled data points, that is, inputs aren't tagged with the resultant output in which the models are needed for finding the patterns from the given training datasets to make predictions. In supervised learning, the training data consists of labels for training the model as well as making predictions. The model could gain knowledge and become more accurate in its prediction by utilizing the training data. Training data is used to stop overfitting.

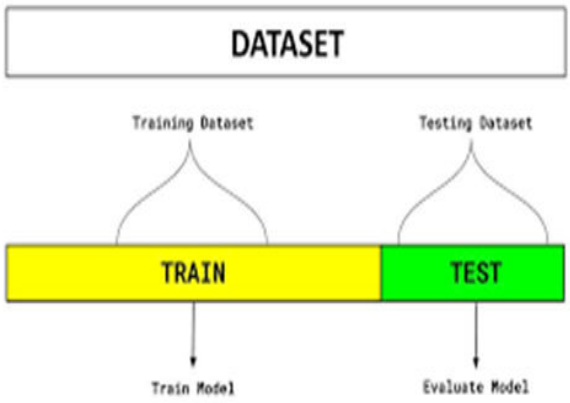

Fig.7. Dataset splitting

By classifying the inputs and outputs, the training dataset is analyzed; next, it is examined again and utilized for building ML models. By utilizing the unseen samples in the testing part, the prediction performance is estimated after training the training part with an ML algorithm. And, the predicted data's outcomes are analogized with the actual value in the testing.

| e-ISSN: 2320-9801, p-ISSN: 2320-9798| www.ijircce.com | |Impact Factor: 8.379 | Monthly Peer Reviewed & Referred Journal |

|| Volume 12, Issue 3, March 2024 ||

| DOI: 10.15680/IJIRCCE.2024.1203009 |

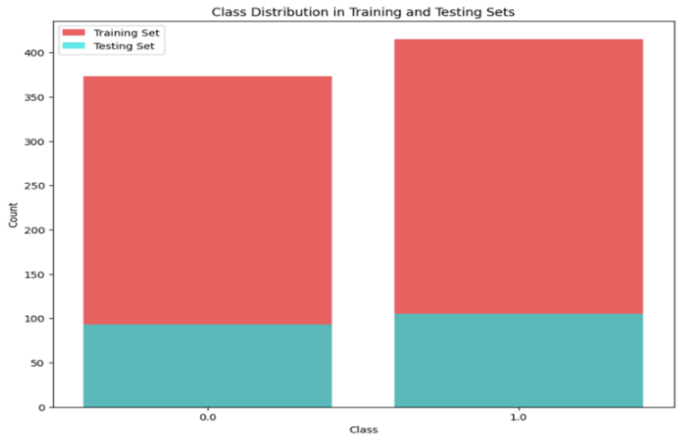

Fig.8. Graphical representation of normal and abnormal data of splitting dataset

g. Training using Random Forest Algorithm

For attaining accuracy and problem-solving ability, an RF algorithm is done under the classification problem. The process that merges multiple classifiers for solving complex issues along with enhancing the model's performance is called ensemble learning. For predicting accuracy, the data works under an RF algorithm after training the model. As exhibited in Figure 6, random samples are selected from the class training set. Now, the model is fitted to the training set for which the DT Classifier is brought in from the sklearn.tree library. The DT is categorized into 2 nodes, namely the decision node as well as leaf node.

For making any decision, decision nodes that have multiple branches are utilized, while leaf nodes are those decisions' output as well as don't enclose any more branches. For the given dataset, the algorithm initiates the class prediction from the tree's root node. The root attribute's value is analogized with the record (real dataset) attribute. Centered on the assessment, this approach follows the branches and jumps to the next node. Again, for the next node, the attribute value is analogized with other sub-nodes and moved further. Till the tree's leaf node is reached, the process is continued. While problems arise in choosing the foremost attribute for the root node and sub-node, the Attribute Selection Measure is utilized for finding the best attribute in the dataset. This is carried out by Information Gain (IG), which measures the variations in entropy subsequent to the dataset segmentation regarding an attribute. Moreover, it estimates how much information regarding a class is rendered by a feature. The node is split, and the DT is built according to the IG value. A DT always tries to increase the IG value. Initially, the attributes that have the topmost IG are split. It is computed by,

Information Gain=Entropy(S)-[(weighted Avg)*Entropy(each feature)]

The impurity in a provided attribute is measured by entropy, which indicates the randomness in data. It is estimated as,

$$Entropy(S)=-P(yes)\log_2 P(yes) - P(no)\log_2 P(no)$$

Here, S=Total number of samples
P(yes)= probability of yes
P(no)= probability of no

This predicts the test set outcomes. Thus, the predicted and real test outputs are obtained. The prediction vector value is dissimilar to the real vector values; also, the classifier performs a few incorrect predictions. For avoiding any overfitting and underfitting of the data and measuring the accuracy, validation is done for the predicted value. The accuracy score attained by the RF algorithm is 82.32.

IV. EXPERIMENTAL RESULTS

a. Results on Gait Stabilization

Here, by utilizing the RF algorithm, gait stabilization is predicted by splitting the dataset that contains multiple datasets using the DT algorithm. While a new data point takes place regarding the majority of outcomes, every single DT yields a prediction outcome. Lastly, the final decision is predicted by the RF classifier. Thus, the accuracy score is attained.

| e-ISSN: 2320-9801, p-ISSN: 2320-9798| www.ijircce.com | |Impact Factor: 8.379 | Monthly Peer Reviewed & Referred Journal |

|| Volume 12, Issue 3, March 2024 ||

| DOI: 10.15680/IJIRCCE.2024.1203009 |

The f1-score, recall, precision, and support of normal and abnormal conditions are represented in the classification report.

Classification Report:

	precision	recall	f1-score	support
0.0	0.79	0.85	0.82	93
1.0	0.86	0.80	0.83	105
accuracy			0.82	198
macro avg	0.82	0.82	0.82	198
weighted avg	0.83	0.82	0.82	198

Fig.9. Classification report of normal and abnormal predictions

Now, for determining the correct as well as incorrect predictions, the confusion matrix is created.

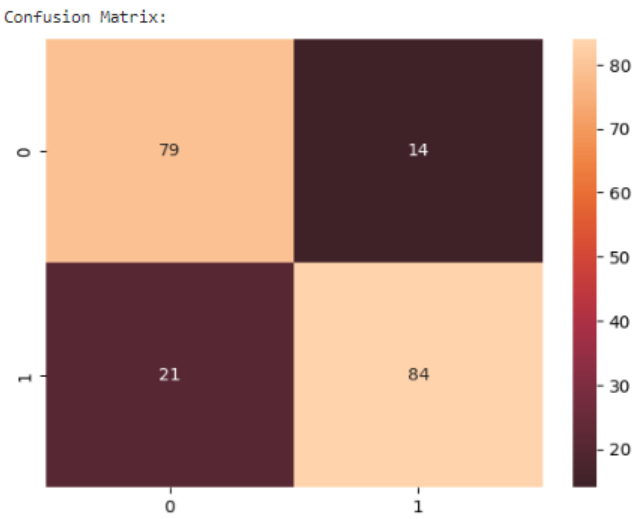

Fig.10. Results on correct and incorrect predictions in the confusion matrix

Correct and incorrect predictions are determined from Figure 7. There are 14+21=35 incorrect predictions and 79+84=163 correct predictions.

The proposed work is analogized with prevailing work, which precedes human subjects in overground walking by achieving the highest accuracy of fall-risk prediction conditions. For predicting the gait instability, the Random Forest ML Algorithm is utilized. It provides more accuracy than the Kalman filter-centric technique utilized in the prevailing model for estimating MoS as well as spatiotemporal gait parameters in real-time. The Kinect sensor is costlier and difficult to implement for real-time usage; so, the accelerometer and gyroscope sensors are utilized in the proposed model to measure the direction and motion of humans more flexibly. By utilizing an algorithm without any overfitting data, more dataset collection could be easily valued. For predicting the gait accuracy in real-time, the proposed model is considered.

b. Limitation and Future work

This model uses wearable instrumented insoles that measure the inertial measurement for fetching the change in the stability of motion while walking and the AI-based prediction. A mobile application will be developed in the future, where the predicted parameters together with gait instability (yes or no) will be displayed. If the gait instability is yes, then the buzzer integrated with the wearable will switch on for alerting the person.

| e-ISSN: 2320-9801, p-ISSN: 2320-9798| www.ijircce.com | |Impact Factor: 8.379 | Monthly Peer Reviewed & Referred Journal |

|| Volume 12, Issue 3, March 2024 ||

| DOI: 10.15680/IJIRCCE.2024.1203009 |

V. CONCLUSION

This work propounded a gait stabilization monitoring system that consists of wearable instrumented insoles. For estimating the prediction in real-time, the RF Algorithm was developed to fuse measurements from the accelerometer and gyroscope sensor on the insoles. The experimental outcomes using this algorithm displayed higher accuracy for gait in normal and abnormal conditions. When analogized with the prevailing work, this algorithm handles a big dataset running with many variables; also, higher accuracy is acquired in gait stabilization prediction. In future work, mobile application development with predicted parameters together with gait instability (yes or no) prediction will be included.

REFERENCES

[1] Zhuo Chen, Huanghe Zhang, Antonia Zaferiou, Damiano Zanotto, and Yi Guo, "Mobile Robot Assisted Gait Monitoring and Dynamic Margin of Stability Estimation," *Sci. Rep.*, vol. 4,no. 2, pp. 1–10, 2022.
[2] K. Karamanidis, A. Arampatzis, and L. Mademli, "Age-related deficit in dynamic stability control after forward falls is affected by muscle strength and tendon stiffness," *J. Electromyogr. Kinesiol.*, vol. 18, no. 6, pp. 980–989, 2008.
[3] A. F. Ambrose, G. Paul, and J. M. Hausdorff, "Risk factors for falls among older adults: A review of the literature," *Maturitas*, vol. 75, no. 1, pp. 51–61, 2013.
[4] S. Whitney, M. Hudak, and G. Marchetti, "The dynamic gait index relates to self-reported fall history in individuals with vestibular dys function," *J. Vestib. Res.*, vol. 10, no. 2, pp. 99–105, 2000.
[5] L. Salonen and S.-L. Kivelä, "Eye diseases and impaired vision as possible risk factors for recurrent falls in the aged: A systematic review," *Curr. Gerontol. Geriatr. Res.*, vol. 2012, Aug. 2012, Art. no. 271481.
[6] J. M. Hausdorff, D. A. Rios, and H. K. Edelberg, "Gait variability and fall risk in community-living older adults: A 1-year prospective study," *Archives Phys. Med. Rehabil.*, vol. 82, no. 8, pp. 1050–1056, 2001.
[7] C. S. Florence, G. Bergen, A. Atherly, E. Burns, J. Stevens, and C. Drake, "Medical costs of fatal and nonfatal falls in older adults," *J. Amer. Geriatr. Soc.*, vol. 66, no. 4, pp. 693–698, 2018.
[8] S. Bruijn, O. Meijer, P. Beek, and J. Van Dieën, "Assessing the stability of human locomotion: A review of current measures," *J. Roy. Soc. Interface*, vol. 10, no. 83, 2013, Art. no. 20120999.
[9] A. Hof, M. Gazendam, and W. E. Sinke, "The condition for dynamic stability," *J. Biomech.*, vol. 38, no. 1, pp. 1–8, 2005.
[10] M. I. M. Refai, B.-J. F. van Beijnum, J. H. Buurke, and P. H. Veltink, "Gait and dynamic balance sensing using wearable foot sensors," *IEEE Trans. Neural Syst. Rehabil. Eng.*, vol. 27, no. 2, pp. 218–227, Feb. 2019.
[11] H. Ohtsu*et al.*, "Does the balance strategy during walking in elderly persons show an association with fall risk assessment?" *J. Biomech.*, vol. 103, Apr. 2020, Art. no. 109657.
[12] F. Franchignoni, F. Horak, M. Godi, A. Nardone, and A. Giordano, "Using psychometric techniques to improve the balance evaluation systems test: The mini-bestest," *J. Rehabil. Med.*, vol. 42, no. 4, pp. 323–331, 2010.
[13] H. Ohtsu, S. Yoshida, T. Minamisawa, T. Takahashi, S.-I. Yomogida, and H. Kanzaki, "Investigation of balance strategy over gait cycle based on margin of stability," *J. Biomech.*, vol. 95, Oct. 2019, Art. no. 109319.
[14] L. Mademli and A. Arampatzis, "Lower safety factor for old adults during walking at preferred velocity," *Age*, vol. 36, no. 3, p. 9636, 2014. [15] M. Guaitolini, F. Aprigliano, A. Mannini, A. Sabatini, and V. Monaco, "Effects of gait speed on the margin of stability in healthy young adults," in *Proc. Int. Conf. NeuroRehabil.*, 2018, pp. 420–424.
[16] F. B. van Meulen, D. Weenk, J. H. Buurke, B.-J. F. Van Beijnum, and P. H. Veltink, "Ambulatory assessment of walking balance after stroke using instrumented shoes," *J. NeuroEng. Rehabil.*, vol. 13, no. 1, p. 48, 2016.
[17] M. Guaitolini, F. Aprigliano, A. Mannini, S. Micera, V. Monaco, and A. M. Sabatini, "Ambulatory assessment of the dynamic margin of stability using an inertial sensor network," *Sensors*, vol. 19, no. 19, p. 4117, 2019.
[18] P. C. Fino, F. B. Horak, and C. Curtze, "Inertial sensor-based centripetal acceleration as a correlate for lateral margin of stability during walking and turning," *IEEE Trans. Neural Syst. Rehabil. Eng.*, vol. 28, no. 3, pp. 629–636, Mar. 2020.
[19] J. F. Veneman, R. Kruidhof, E. E. Hekman, R. Ekkelenkamp, E. H. Van Asseldonk, and H. Van Der Kooij, "Design and evaluation of the LOPES exoskeleton robot for interactive gait rehabilitation," *IEEE Trans. Neural Syst. Rehabil. Eng.*, vol. 15, no. 3, pp. 379–386, Sep. 2007.
[20] R. A. R. C. Gopura, K. Kiguchi, and Y. Li, "SUEFUL-7: A 7DOF upper-limb exoskeleton robot with muscle-model-oriented Emg-based control," in *Proc. IEEE/RSJ Int. Conf. Intell. Robots Syst. (IROS)*, 2009, pp. 1126–1131.
[21] G. Chalvatzaki, P. Koutras, J. Hadfield, X. S. Papageorgiou, C. S. Tzafestas, and P. Maragos, "LSTM-based network for human gait stability prediction in an intelligent robotic rollator," in *Proc. IEEE Int. Conf. Robot. Autom. (ICRA)*, 2019, pp. 4225–4232.
[22] H. Zhang, Z. Chen, D. Zanotto, and Y. Guo, "Robot-assisted and wear able sensor-mediated autonomous gait analysis," in *Proc. IEEE Int. Conf. Robot. Autom. (ICRA)*, 2020, pp. 6795–6802.

| e-ISSN: 2320-9801, p-ISSN: 2320-9798| www.ijircce.com | |Impact Factor: 8.379 | Monthly Peer Reviewed & Referred Journal |

|| Volume 12, Issue 3, March 2024 ||

| DOI: 10.15680/IJIRCCE.2024.1203009 |

[23] H. Zhang, D. Zanotto, and S. K. Agrawal, "Estimating CoP trajectories and kinematic gait parameters in walking and running using instrumented insoles," *IEEE Robot. Autom. Lett.*, vol. 2, no. 4, pp. 2159–2165, Oct. 2017.
[24] H. Zhang, Y. Guo, and D. Zanotto, "Accurate ambulatory gait analysis in walking and running using machine learning models," *IEEE Trans. Neural Syst. Rehabil. Eng.*, vol. 28, no. 1, pp. 191–202, Jan. 2020.
[25] "Documentation for Azure Kinect DK." [Online]. Available: https://docs.microsoft.com/en-us/azure/Kinect-dk/ (Accessed: Oct. 13, 2020).
[26] M. Labbé and F. Michaud, "RTAB-Map as an open-source lidar and visual simultaneous localization and mapping library for large-scale and long-term Online operation," *J. Field Robot.*, vol. 36, no. 2, pp. 416–446, 2019.
[27] D. Fox, W. Burgard, and S. Thrun, "The dynamic window approach to collision avoidance," *IEEE Robot. Autom. Mag.*, vol. 4, no. 1, pp. 23–33, Mar. 1997.
[28] J. Perry and J. R. Davids, "Gait analysis: Normal and pathological function," *J. Pediatr. Orthop.*, vol. 12, no. 6, p. 815, 1992. [32] J. Sola, "Quaternion kinematics for the error-state Kalman filter," 2017, *arXiv:1711.02508*.
[29] B. J. Stephens, "State estimation for force-controlled humanoid balance using simple models in the presence of modeling error," in *Proc. IEEE Int. Conf. Robot. Autom. (ICRA)*, 2011, pp. 3994–3999.
[30] R. L. Graham, "An efficient algorith for determining the convex hull of a finite planar set," *Inf. Process. Lett.*, vol. 1, no. 4, pp. 132–133, 1972. [35] T. K. Koo and M. Y. Li, "A guideline of selecting and reporting intraclass correlation coefficients for reliability research," *J. Chiropr. Med.*, vol. 15, no. 2, pp. 155–163, 2016.
[31] M. Kazanski, J. P. Cusumano, and J. B. Dingwell, "Rethinking mar gin of stability: Incorporating step-to-step regulation to resolve the paradox," *bioRxiv (The Preprint Server for Biology)*, Dec. 2021, doi: 10.1101/2021.12.01.470263.

INNO SPACE
SJIF Scientific Journal Impact Factor

Impact Factor: 8.379

doi cross ref

ISSN INTERNATIONAL STANDARD SERIAL NUMBER INDIA

निस्केयर NISCAIR

INTERNATIONAL JOURNAL OF INNOVATIVE RESEARCH

IN COMPUTER & COMMUNICATION ENGINEERING

9940 572 462 6381 907 438 ijircce@gmail.com

www.ijircce.com

Scan to save the contact details